



OPEN **Bufei Yishen formula alleviates airway epithelial cell senescence in COPD by activating AMPK-Sirt1-FoxO3a pathway and promoting autophagy**

Mengmeng Cheng^{1,2,5}, Miao Yang^{1,2,5}, Yange Tian^{1,2,3}, Xinguang Liu^{1,2,3}, Jiansheng Li^{1,2,4}✉ & Peng Zhao^{1,2,3}✉

The Bufei Yishen formula (BYF) has traditionally been employed to treat patients with COPD, demonstrating significant effectiveness. However, the underlying mechanisms through which BYF alleviates COPD remains unclear. Cellular senescence is crucial in the pathogenesis of COPD. This study aims to investigate whether the therapeutic mechanism of BYF is associated with the reduction of cellular senescence. To evaluate the anti-senescence effects of BYF, a COPD rat model and a cellular senescence model were established. The active compounds and underlying mechanisms of BYF were investigated in vitro. BYF treatment significantly mitigated lung function decline and pathological damage in COPD rats. It significantly inhibited senescence in lung tissue by decreasing the expression of the cell cycle inhibitor p21, DNA damage markers, pro-inflammatory cytokines, and matrix metalloproteinases. BYF4/5, isolated from BYF, demonstrated significant anti-senescence effects in bronchial epithelial cells. Additionally, 67 compounds were identified from BYF4/5, and 770 targets were predicted for these compounds. hesperidin and nobiletin, identified as key compounds in BYF, were found to inhibit cellular senescence and activate the AMPK-Sirt1-FoxO3a pathway and autophagy in 16HBE cells. The data indicate that BYF alleviates COPD by activating the AMPK-Sirt1-FoxO3a pathway and autophagy, thereby inhibiting bronchial epithelial cell senescence.

Keywords Bufei Yishen formula, Chronic obstructive pulmonary disease, Cellular senescence, Autophagy, AMPK, Sirt1, FoxO3a

Abbreviations

ANOVA	Analysis Of Variance
BWT	Bronchial Wall Thickness
BYF	Bufei Yishen Formula
COPD	Chronic obstructive pulmonary disease
CSE	Cigarette Smoke Extract
EF50	Expiratory Flow at 50% tidal volume
IF	Immunofluorescence technique
IHC	Immunohistochemical staining
IOD	Integrated Optical Density
KEGG	Kyoto Encyclopedia of Genes and Genomes
LSD	Least Significant Difference

¹Henan Key Laboratory of Chinese Medicine for Respiratory Disease, Henan University of Chinese Medicine, 156 Jinshui Dong Road, Zhengzhou 450046, Henan, China. ²Collaborative Innovation Center for Chinese Medicine and Respiratory Diseases Co-Constructed By Henan Province & Education Ministry of People's, Zhengzhou, Republic of China. ³Academy of Chinese Medical Sciences, Henan University of Chinese Medicine, Zhengzhou 450046, Henan, China. ⁴Department of Respiratory Diseases, the First Affiliated Hospital of Henan University of Chinese Medicine, Zhengzhou 450000, China. ⁵Mengmeng Cheng and Miao Yang These authors are contributed equally. ✉email: li_js8@163.com; zhaopeng871@126.com

LPS	Lipopolysaccharide
MMP	Matrix Metalloproteinase
MAN	Mean Alveolar Number
MLI	Mean Linear Intercept
MV	Minute Volume
PEF	N-acetylcysteine (NAC) Peak Expiratory Flow
SASP	Senescence-Associated Secretory Phenotype
SA- β -Gal	Senescence-Associated β -Galactosidase
SIRT1	Sirtuin1
TV	Tidal Volume
TCM	Traditional Chinese Medicine

Chronic obstructive pulmonary disease (COPD) is a heterogeneous respiratory disorder characterized by persistent respiratory symptoms and partially reversible airflow limitation¹. COPD significantly impacts both the economy and society, imposing a considerable burden in terms of morbidity and mortality rates². Cigarette smoke along with other stimuli such as wood and biomass combustion smoke, are the primary risk factors for COPD. These irritants often elicit inflammatory responses and lead to oxidative stress injury, disrupting the balance between proteases and antiproteases, resulting in various pathological changes such as chronic bronchitis, small airway disease, or emphysema^{3–5}. However, the primary therapeutic strategies for COPD, including bronchodilators and anti-inflammatory agents, do not exhibit satisfactory efficacy on these pathological changes. Therefore, new mechanisms underlying the development of COPD and effective therapeutics urgently require further investigation.

The airway epithelium, serving as the primary protective barrier against inhaled exogenous irritants, plays a key role in the onset of COPD⁶. Continuous exposure to tobacco smoke leads to persistent chronic inflammation and damage to lung tissues, partially attributed to the accumulation of senescent cells. Specifically, airway epithelial cellular senescence tends to accumulate within the lungs of individuals with COPD^{7,8}. Cigarette smoke-induced airway epithelial cellular senescence displays various markers, including irreparable DNA damage, oxidative stress, expression of senescence-associated β -galactosidase, cell cycle inhibitors (such as p16 and p21), and the tumor suppressor p53, as well as the release of the senescence-associated secretory phenotype (SASP), characterized by highly expressed pro-inflammatory cytokines, chemokines, matrix metalloproteinases^{9–12}. Many oral nutritional supplements such as the antioxidants resveratrol, vitamin C, vitamin D, eicosapentaenoic acid, and polyunsaturated fatty acids, exhibit significant anti-senescence effects. Additionally, these oral nutritional supplements can optimize the nutritional status, increase body weight, improve muscle strength and physical function, enhance inspiratory muscle strength, alleviate dyspnea, increase total protein concentration, and reduce the inflammatory response, leading to improved quality of life and overall survival in COPD patients¹³. AMP-activated protein kinase (AMPK) functions as a metabolic sensor that is activated by cellular stress. By restoring energy homeostasis and promoting cellular autophagy and repair mechanisms, AMPK plays a vital role in delaying the onset of cellular senescence^{14,15}. The pivotal role of SIRT1 in regulating cellular senescence is underscored by its effects on maintaining genomic stability and reducing cellular stress¹⁶. For instance, SIRT1 can activate FOXO3a and enhance its ability to bind DNA, inducing the expression of antioxidant genes¹⁷. Moreover, AMPK activation can increase the NAD⁺/NADH ratio, which in turn activates SIRT1 by providing its co-substrate, NAD⁺¹⁸. Thus, activating the AMPK-SIRT1 pathway to combat cellular senescence is a promising strategy to alleviate COPD.

Traditional Chinese medicine is widely used to alleviate symptoms of COPD without significant side effects. Bufei Yishen formula (patent: ZL.201110117578.1) is specifically prescribed for COPD patients exhibiting lung-kidney qi deficiency syndrome and comprises twelve medicinal herbs^{19,20}. Previous clinical studies have demonstrated that six months of treatment with BYF can effectively improve COPD symptoms, including reducing exacerbation frequency, and improving pulmonary function and exercise capacity²¹. Subsequent animal studies showed that BYF treatment maintains airway epithelial barrier function by upregulating apical junction proteins and reducing epithelial permeability in rats with COPD and in cigarette smoke-exposed epithelial cells²². Nevertheless, the alleviation effect of BYF on airway epithelial cellular senescence remains to be elucidated. Therefore, this investigation aimed to explore the inhibitory effects of BYF on epithelial cellular senescence in COPD rats and epithelial cells induced by cigarette smoke. Furthermore, this study delved into the underlying mechanisms and key components of BYF that effectively prevent epithelial cell senescence through network analysis and transcriptomics. The findings of this research will enhance our understanding of the potential therapeutic benefits of this herbal formula in treating COPD.

Results

BYF attenuates lung function decline and pathological damage in COPD rats

To evaluate the protective effects of BYF, we established a rat model of COPD by exposing the rats to cigarette smoke and bacterial infection from week 1 to 8. BYF's therapeutic effects were assessed at the end of week 16. As shown in Fig. 1, the COPD rats exhibited a significant decline in lung function, including reductions in TV, MV, PEF, and EF50, as well as notable pathological changes in the lungs, such as alveolar structural damage, decreased alveolar number, and increased alveolar diameter and bronchial wall thickness. However, oral BYF treatment obviously suppressed the decrease in lung function and alleviated pathological alterations. These data suggest that BYF treatment can improve COPD in rats by protecting against lung damage and enhancing lung function.

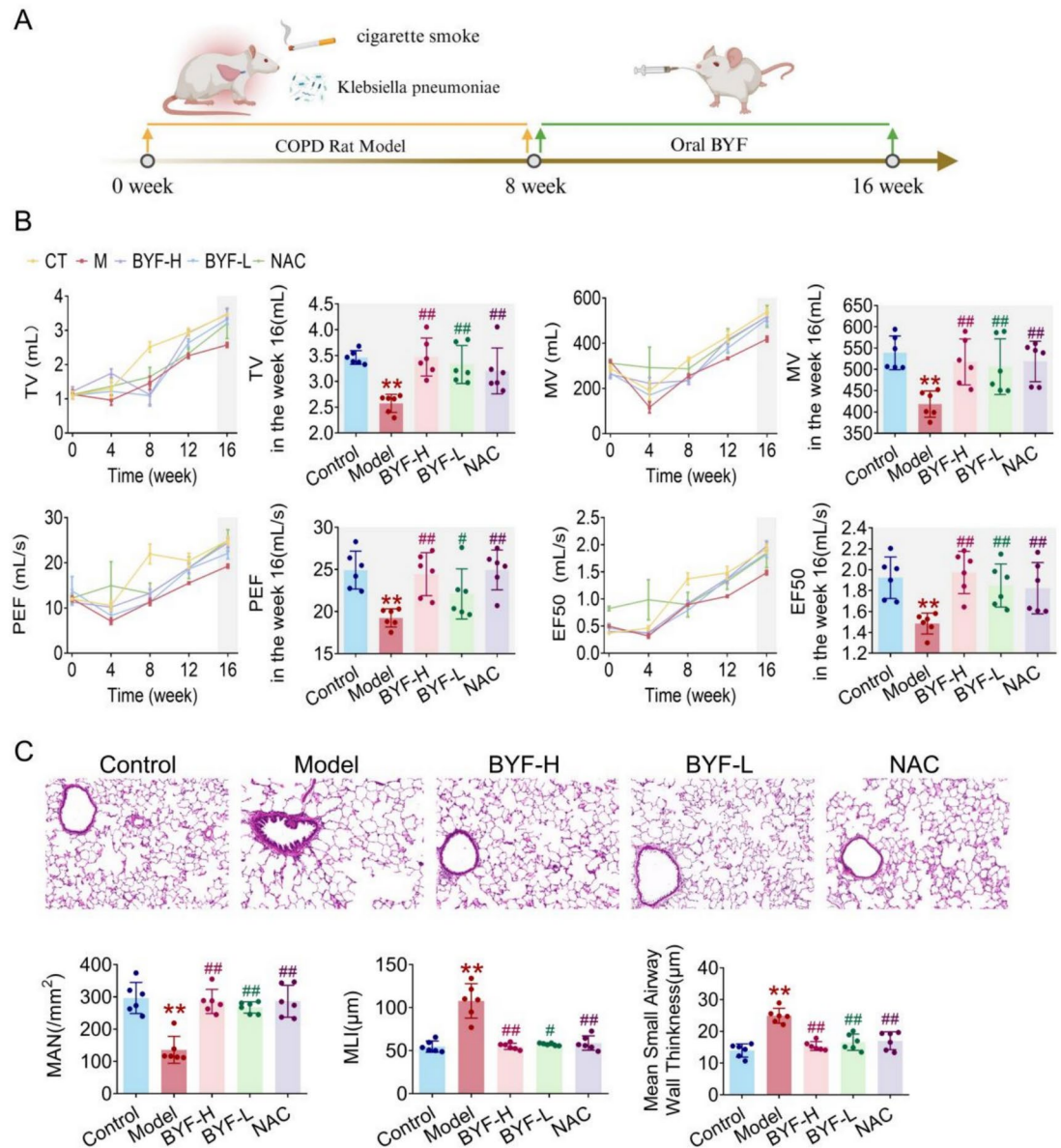


Fig. 1. The Bufei Yishen formula improves pulmonary function and pathological changes in COPD rats. BYF (11.6, 5.8 g/kg) and N-acetylcysteine (NAC, 54 mg/kg) were administered to COPD rats for 9 to 16 weeks. **(A)** Flow chart of the animal experiment. **(B)** Lung function including tidal volume (TV), minute volume (MV), peak expiratory flow (PEF), and expiratory flow at 50% tidal volume (EF50). **(C)** Pathological changes in pulmonary tissue (H&E, $\times 200$) and its quantitative analysis, including mean alveolar number (MAN), mean linear intercept (MLI), and mean small airway wall thickness. Values are expressed as the mean \pm SEM ($n = 6$), * $P < 0.05$, ** $P < 0.01$ compared with the control group; # $P < 0.05$, ## $P < 0.01$ compared with the model group.

BYF suppressed the cellular senescence in the lungs of COPD rats

Cellular senescence is characterized by cell cycle arrest, potential apoptosis, and the emergence of a senescence-associated secretory phenotype (SASP). This phenotype results in the secretion of pro-inflammatory cytokines and proteases, which can propagate senescence within tissues. Consequently, the effects of BYF on the levels of pro-inflammatory cytokines, proteases, and antioxidant proteins were investigated. The data showed that BYF treatment significantly decreased the levels of IL-6, IL-1 β , TNF- α , MMP-2, and MMP-9, while increasing SOD2 expression in lung tissues and serum (Fig. 2, 3A). BYF treatment markedly upregulated the protein expression levels of E-Cadherin (E-CAD), Occludin (OCC), and Zonula Occludens-1 (ZO-1), suggesting that oral administration of BYF can mitigate airway epithelial damage in COPD rats (Fig. 3B). Additionally, BYF increased the expression level of surfactant protein A (SP-A) in rat lung tissue. The findings also indicated that BYF up-regulated the expression of PINK1, a mitophagy marker, in rat lung tissues. In addition, BYF decreased the levels of p21, a protein that inhibits the cell cycle, as well as markers of DNA damage (γ H2 AX and TUNEL) in lung tissues (Fig. 4, 5). Simultaneously, BYF treatment enhanced the expression of the cell proliferation

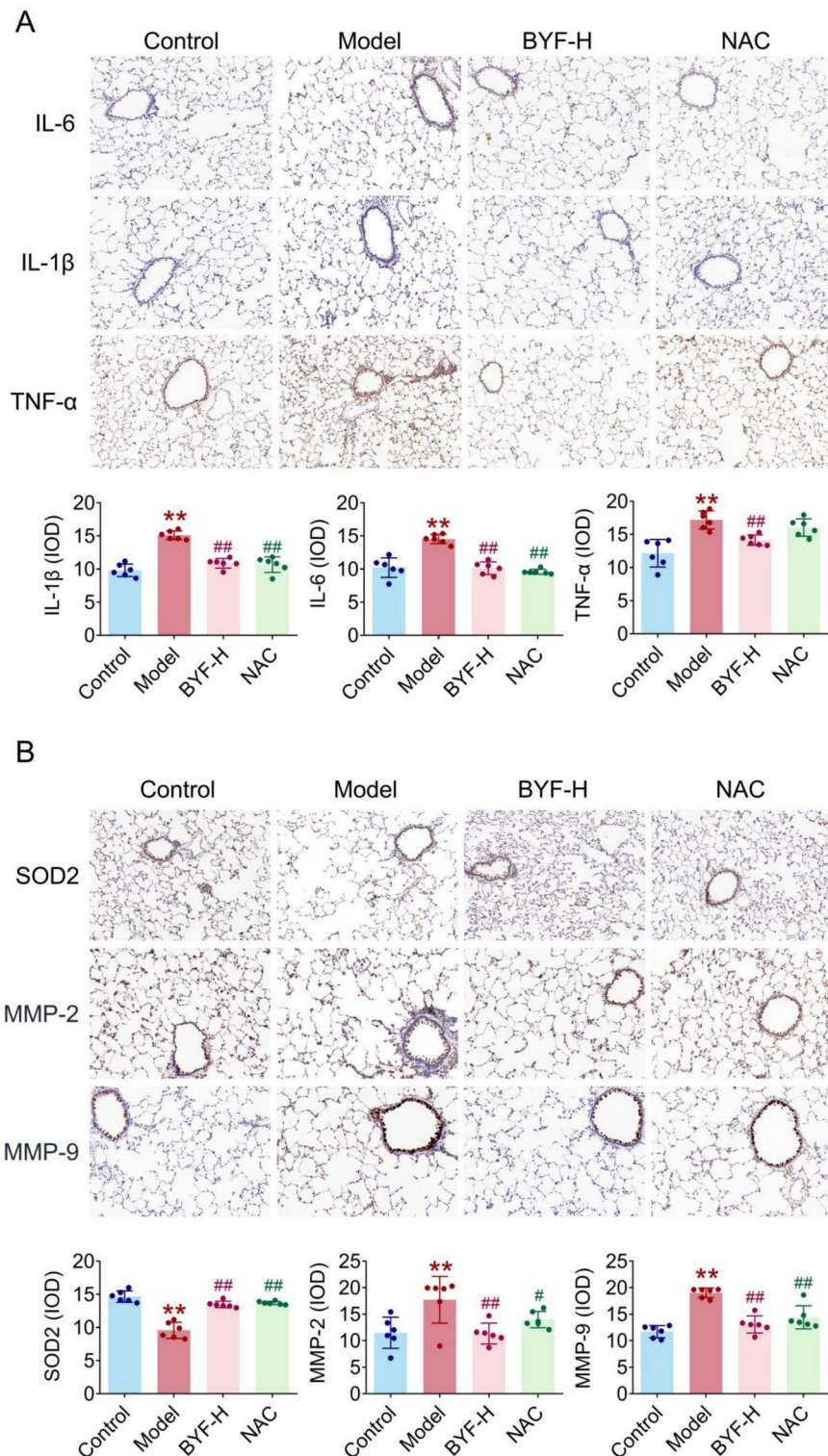


Fig. 2. The Bufei Yishen formula inhibits inflammation, oxidative stress, and protease expression in COPD rats. **(A)** Expression of IL-1 β , IL-6 and TNF- α in lung tissue were detected using the immunohistochemical method and quantified as their integral optical density (IOD). **(B)** The expression of SOD2, MMP-2, and MMP-9 were detected by using immunohistochemical method and quantified as their integral optical density (IOD). Values are expressed as the mean \pm SEM (n = 6), *P < 0.05, **P < 0.01 compared with the control group; #P < 0.05, ##P < 0.01 compared with the model group.

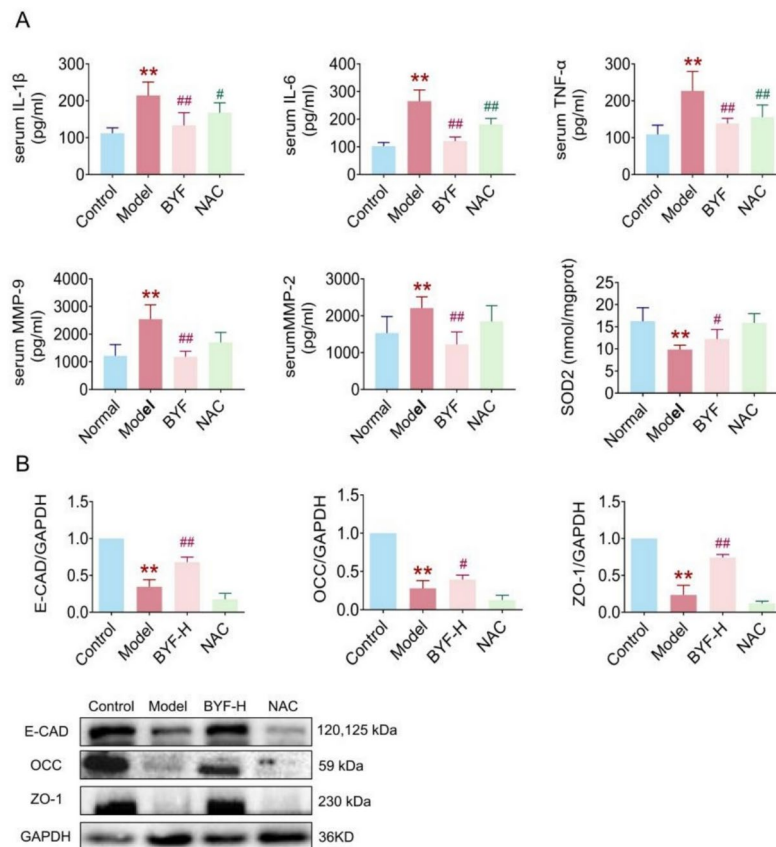


Fig. 3. The Bufei Yishen formula inhibits inflammation, oxidative stress, and protease expression in COPD rats. **(A)** The levels of IL-1 β , IL-6, TNF- α , SOD2, MMP-2, and MMP-9 were measured using ELISA. **(B)** Protein levels of E-CAD, OCC and ZO-1 in lung tissue of rats. Values are expressed as the mean \pm SEM (n = 6), *P < 0.05, **P < 0.01 compared with the control group; #P < 0.05, ##P < 0.01 compared with the model group.

marker Ki67 in lung tissues. These data suggest that oral administration of BYF could alleviate senescence in the lungs of COPD rats.

BYF inhibited cellular senescence in CSE-induced bronchial epithelial cells

Increased senescent cells have been observed in the lung tissues of patients with COPD and are heavily involved in COPD pathogenesis. Bronchial epithelial cells, which serve as the primary cellular defense mechanism against exogenous irritants such as cigarette smoke and bacterial infection, are major contributors to cellular senescence. Thus, 16HBE cells were exposed to BYF1 ~6 (BYF was purified and separated into six fractions) for 3 h, followed by exposure to 10% CSE and 100 ng/mL LPS for 24 h. As shown in Fig. 6A-B, BYF-4 and BYF-5 markedly inhibited the protein expression of p21. Additionally, the combination of BYF-4 and BYF-5 fractions, referred to as BYF4/5, exhibited no significant impact on cell viability across concentrations of 12.5 to 400 μ g/mL. Furthermore, BYF4/5 significantly suppressed both mRNA and protein levels of p53 and p21 (Fig. 6C-F). BYF4/5, identified as the effective component of BYF, was utilized in the vitro experiments.

To further investigate the antisenescent effect of BYF4/5, we evaluated the pro-inflammatory cytokines, chemokines, proteases and β -galactosidase. Figure 5 shows that BYF4/5 treatment significantly decreases the mRNA expression levels of IL-1 α , IL-1 β , TNF- α , CXCR2, CXCL8, MCP-1, MMP-1, MMP-8, and MMP-9, and inhibits the activity of β -galactosidase (Fig. 7). These findings suggest that BYF4/5 could significantly reduce senescence in bronchial epithelial cells.

Network analysis of BYF's antisenescent mechanisms

Firstly, 67 compounds present in BYF4/5, the active fraction of BYF, were identified using UPLC-Q-Exactive-Orbitrap MS (Fig. 8A). Subsequently, 770 targets were predicted for these 67 compounds. To investigate the antisenescent mechanisms of BYF, these 770 targets, along with 317 differentially expressed genes regulated by CSE/LPS in 16HBE cells, were used to construct the PPI network. The PPI network, illustrated in Fig. 8B-F, comprised a total of 943 nodes. KEGG pathway analysis of 157 core nodes (degree value \geq 70) indicated that the p53, FoxO, TNF, NF-kappa B, chemokine, AMPK, Hippo signaling pathways, as well as cellular senescence, cell cycle, and autophagy, might be involved in the antisenescent effect of BYF (Fig. 8G). Furthermore, a Sankey diagram was constructed to visualize the relationships among compounds, targets, and pathways. The results

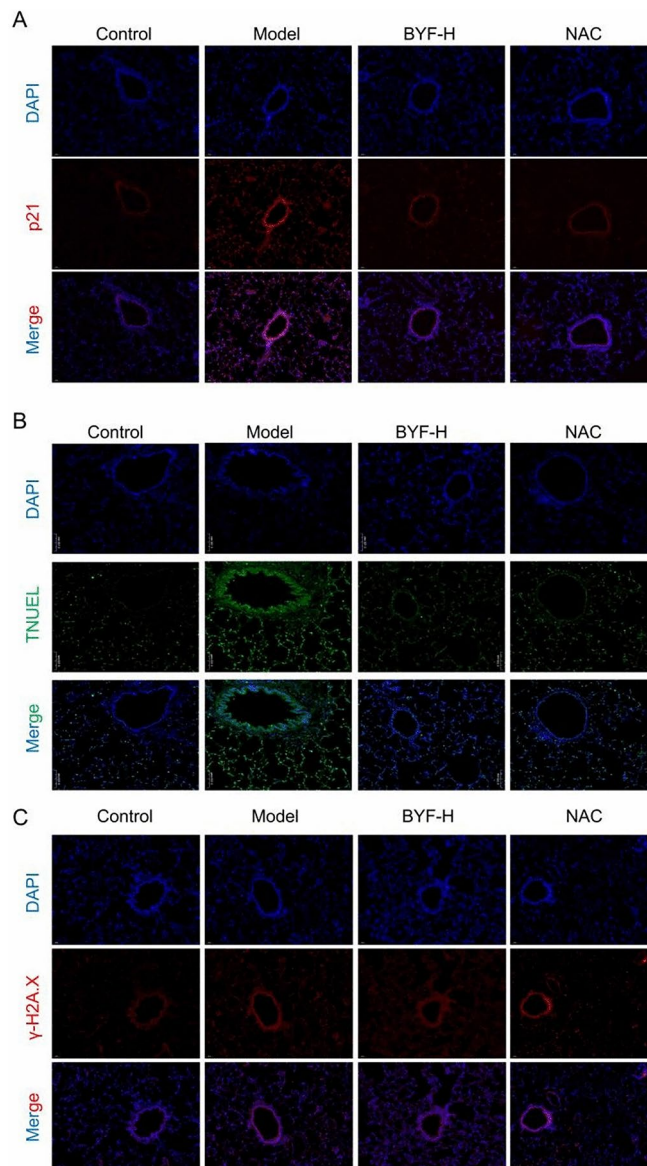


Fig. 4. Effect of Bufei Yishen formula on the protein levels of p21 and γ -H2 AX, as well as cellular apoptosis in the lung tissues of COPD rats. Immunofluorescence staining was applied to detect the p21 (A), TUNEL (B), and γ -H2 AX (C) in lung tissues.

showed that hesperidin, bergenin, peimisine, peimine A, and nobiletin, among others, bound to CDK2, AKT1, AKT2, and other proteins implicated in cellular senescence, FoxO, autophagy, and related processes (Fig. 8H).

The active components of BYF4/5 inhibited cellular senescence and activated AMPK-Sirt1-FoxO3a-mediated autophagy

The results demonstrate that BYF4/5 contains various compounds, including hesperidin and nobiletin, which target multiple proteins implicated in regulating different pathways, such as AMPK, FoxO3a, and autophagy. Previous studies have shown that AMPK, Sirt1, FoxO3a, and autophagy participate in regulating senescence. As illustrated in Fig. 9, hesperidin and nobiletin significantly inhibit the expression of p21 and p53 at both mRNA and protein levels, as well as IL-1 α , IL-1 β , and MMP-9 mRNA levels. Nobiletin (2.5–40 μ g/mL) and hesperidin (10–100 μ g/mL) had no significant effect on cell viability. Furthermore, they effectively suppress β -galactosidase activity. Additionally, hesperidin and nobiletin markedly upregulate phosphorylated AMPK protein levels, Sirt1, and LC3B II, while downregulating FoxO3a phosphorylation and HDAC mRNA expression (Fig. 10). In vivo experiments demonstrated that BYF significantly reduced the protein expression levels of FoxO3a while markedly enhancing the expression of AMPK, SIRT1, and LC3 in rat lung tissue (Fig. 11, Fig. 12). These findings suggest that the active compounds in BYF can suppress cellular senescence by potentially activating the AMPK-Sirt1-FoxO3a pathway and autophagy.

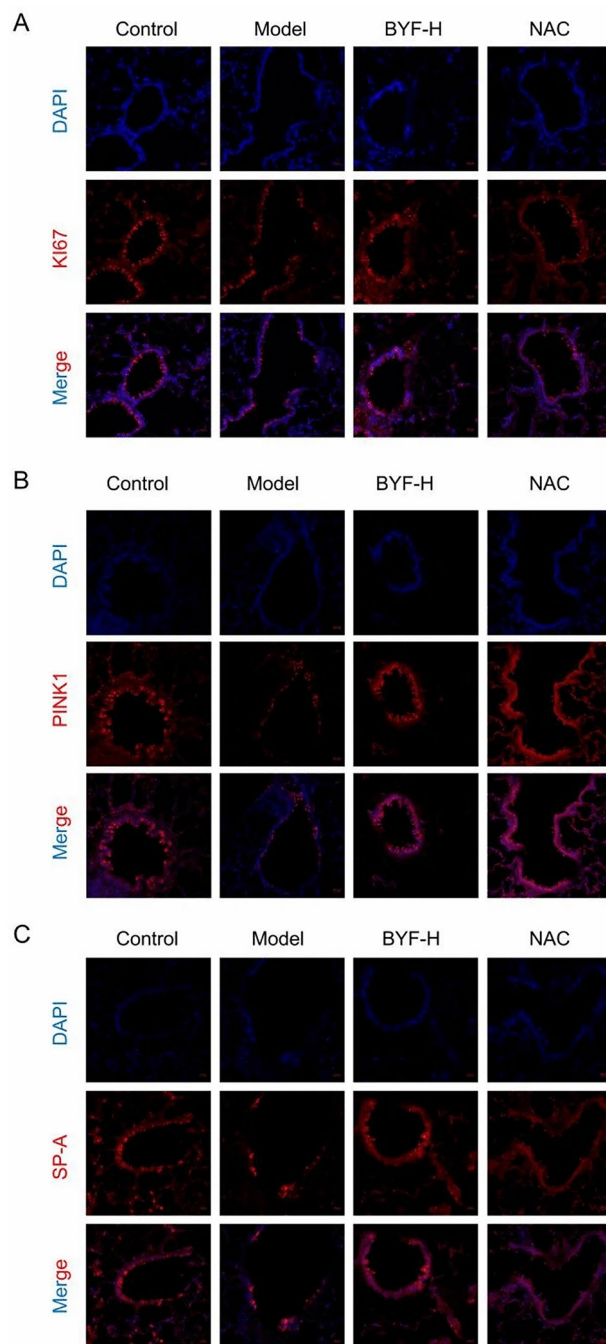


Fig. 5. Effect of Bufei Yishen formula on the protein levels of Ki67, PINK1 and SP-A in the lung tissues of COPD rats. Immunofluorescence staining was applied to detect the Ki67 (A), PINK1 (B), and SP-A (C) in lung tissues.

Discussion

COPD represents a significant public health challenge due to its widespread occurrence and significant financial impact²³. Current therapeutic strategies available for treating COPD, such as corticosteroids and bronchodilators, have demonstrated limited efficacy. BYF, prescribed for COPD patients with lung-kidney qi deficiency syndrome, has exhibited unique benefits in reducing the exacerbation frequency and improving lung function and exercise capacity²⁴. For instance, randomized controlled trials have been demonstrated that BYF, as compared to a placebo, could significantly reduce the frequent acute exacerbations and their related hospitalizations for GOLD 3–4 COPD patients, improved clinical symptoms, treatment satisfaction, quality of life, and exercise capacity²⁵. In another clinical study, patients treated with conventional western medicine in conjunction with BYF experienced a reduction in the frequency and duration of AECOPD, alleviated symptoms, and improved exercise tolerance²¹. However, the mechanism of improving COPD by BYF is still unclear, especially the effect

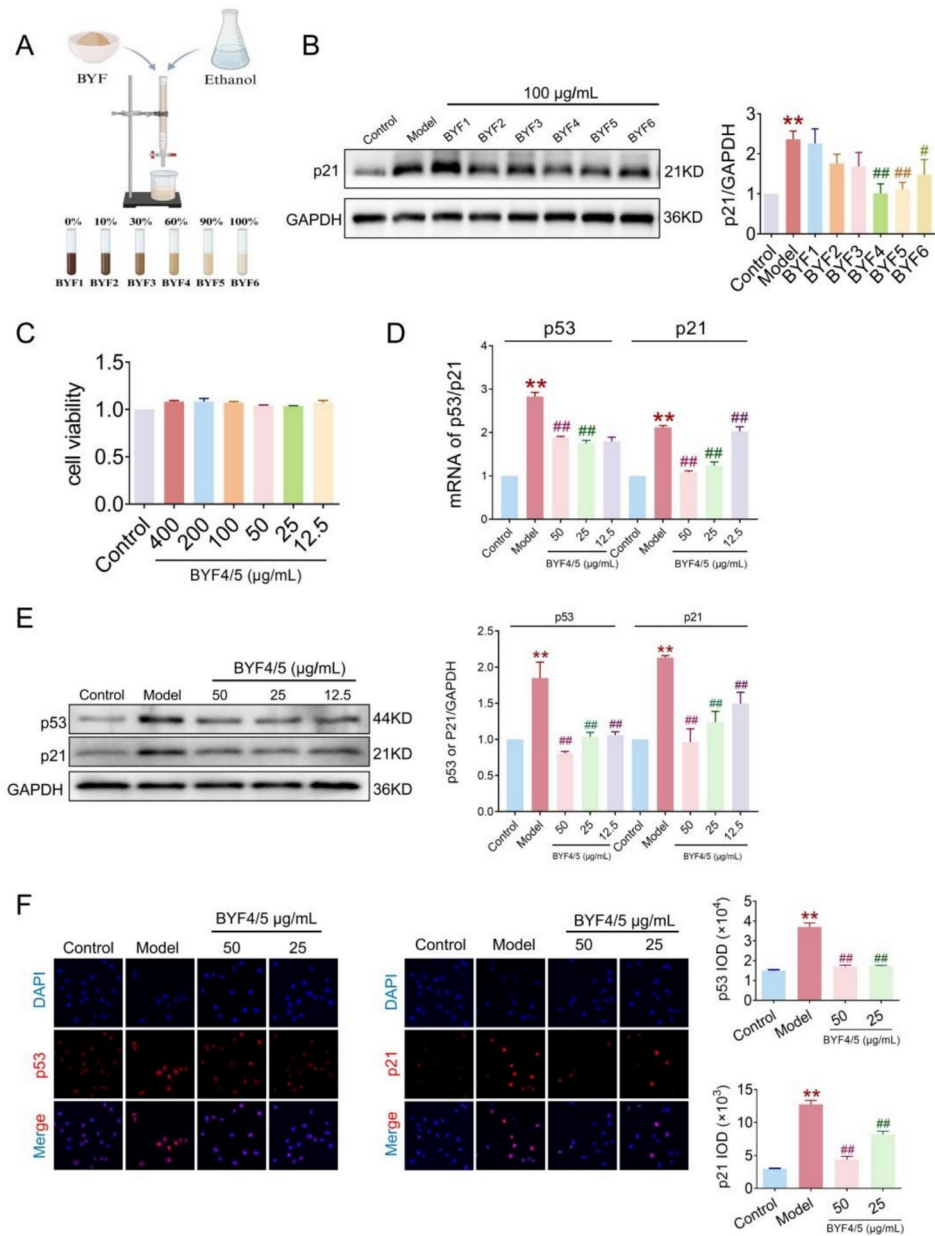


Fig. 6. Effect of Bufei Yishen formula 1 ~ 6 on cigarette smoke extract (CSE)- and LPS-induced 16-HBE cells. (A) Flow chart of BYF isolation. (B) Protein levels of p21 in BYF1–6-treated 16-HBE cells induced by CSE/LPS. (C) The impact of BYF4/5 on cell viability (D) The mRNA levels of p53 and p21. (E) Protein levels of p53 and p21 in BYF4/5-treated 16-HBE cells induced by CSE/LPS. (F) The protein levels of p53 and p21 in 16HBE cells were detected by immunofluorescence staining. Values are expressed as the mean \pm SEM (n = 3), *P < 0.05, **P < 0.01 compared with the control group; #P < 0.05, ##P < 0.01 compared with the model group.

and mechanism on senescence. In this study, we confirmed that oral BYF treatment mitigated lung function decline, pathological alterations, inflammatory response, protease levels, and senescence markers in COPD rats. Moreover, BYF and its active compounds showed a notable anti-senescence effect on airway epithelial cells, potentially through the activation of the AMPK-Sirt1-FoxO3a signaling pathway and autophagy. These results underscore the therapeutic potential of BYF in managing COPD and propose it as a viable treatment strategy.

Chronic obstructive pulmonary disease (COPD) is highly prevalent in older adults. The incidence of COPD increases with age, with a prevalence rate of 8.6% in the Chinese population aged ≥ 20 years and rising to 13.7% in those aged ≥ 40 years. Aging has a significant impact on the development of COPD²⁶. “Aging” refers to the progressive decline in tissue homeostasis due to aging, leading to increased susceptibility to diseases and organ failure, caused by continued oxidative stress-induced DNA damage (premature senescence) or replication exhaustion caused by telomere shortening (replicative senescence). Environmental stressors, such as cigarette smoke or other pollutants, may accelerate lung cell aging through oxidative stress, thus advancing the progression of COPD⁹. Cellular senescence refers to the cell cycle arrest and loss of replicative ability, resulting

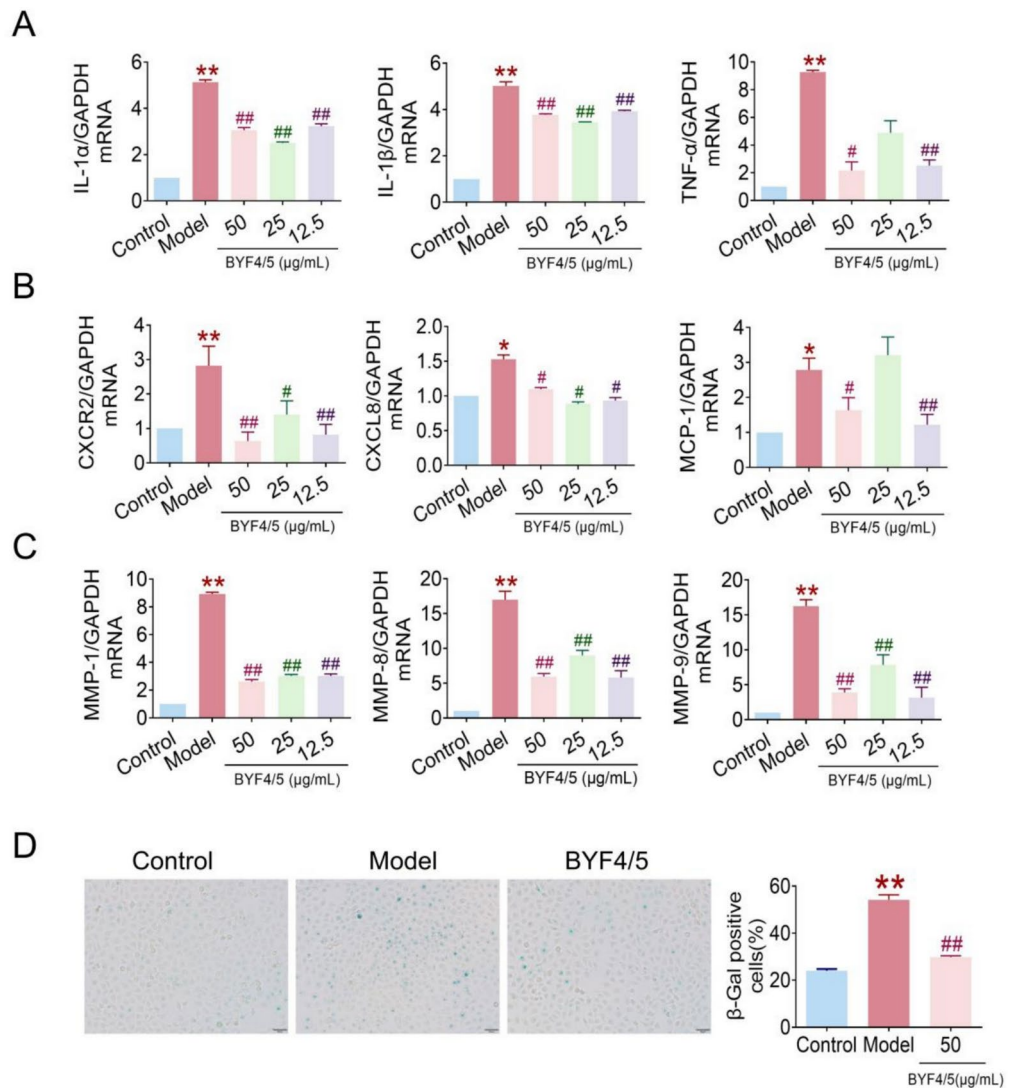


Fig. 7. Effect of Bufei Yishen formula 4/5 on senescence in cigarette smoke extract (CSE)- and LPS-induced 16-HBE cells. (A) The mRNA levels of IL-1 α , IL-1 β and TNF- α . (B) The mRNA levels of CXCR2, CXCL8 and MCP-1. (C) The mRNA levels of MMP-1, MMP-8, and MMP-9. (D) The activity of β -galactosidase. Values are expressed as the mean \pm SEM (n = 3), *P < 0.05, **P < 0.01 compared with the control group; #P < 0.05, ##P < 0.01 compared with the model group.

in tissue inflammation, injury, and loss of their physiological function²⁷. Senescent cells remain metabolically active and perpetuate senescence in themselves and neighboring cells by secreting SASP^{28,29}, which includes proinflammatory cytokines, chemokines, and matrix metalloproteinases (MMPs). Accumulating evidence shows that various senescence markers, such as DNA damage markers (p21, γ H2 AX) and senescent-associated β -galactosidase (SA- β -gal) activity³⁰, are highly expressed in lung tissues of animals exposed to cigarette smoke and COPD patients. For instance, p53 and p21 have been shown to be overexpressed, inducing bronchial epithelial cell senescence in COPD^{31,32}, affecting airway homeostasis, repair, and regeneration and maintaining the persistent inflammation^{33,34}. In this work, BYF treatment significantly improved the lung function and pathological changes. It also inhibited senescence, by suppressing the pro-inflammatory cytokines (IL-16, IL-1 β , TNF- α) and protease (MMP-2 and MMP-9), and increasing SOD2 expression, as well as decreasing p21, γ H2 AX, and TUNEL in the lung tissues of rats with COPD. Senescence of airway epithelial cells holds a pivotal position in the progression of COPD³⁵. Our previous study showed that airway epithelial cells exhibit marked senescence induced by cigarette smoke and LPS^{22,36}. Here, we found that BYF also decreased the levels of p21 and p53 proteins in CSE/LPS-challenged epithelial cells. These results indicate that BYF treatment could improve COPD-related senescence in vivo and in vitro.

BYF consists of 12 Chinese herbal drugs that include thousands of compounds, some of which may actively suppress senescence. Prior to investigating the molecular mechanisms, an analysis of the compounds within BYF is necessary³⁷. Firstly, BYF is categorized into six fractions (BYF1 ~6), with BYF4 and BYF5 showing significant potential in inhibiting cell senescence in vitro. A total of sixty-seven compounds were isolated from

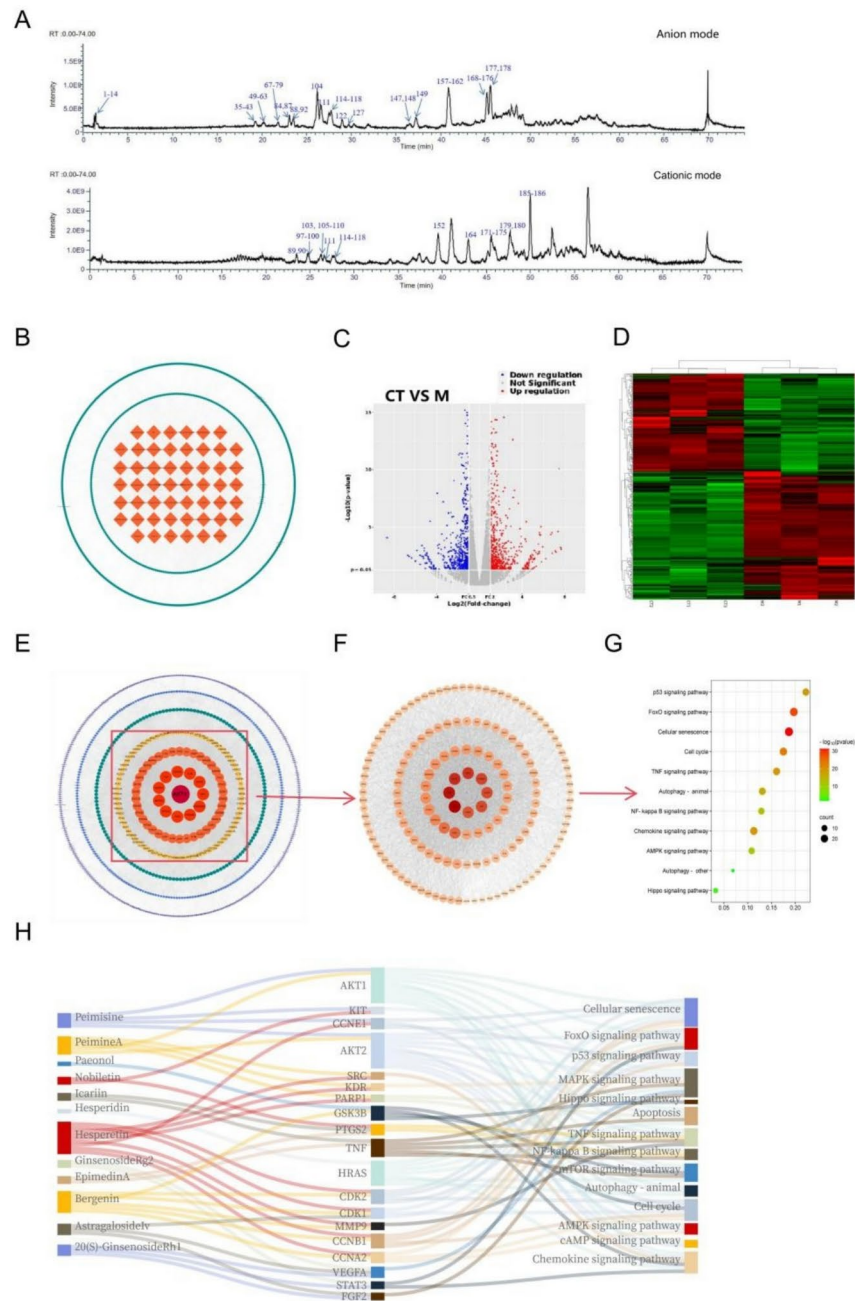


Fig. 8. Network analysis of the anti-senescence mechanisms of Bufei Yishen formula. (A) UHPLC Q-Extractive Orbitrap-MS/MS was used to identify the compounds of the BYF4/5. (B) The compound and target network have been constructed. (C) volcano map (C) and cluster heatmap (D) were applied to showed the DEGs. (E) The PPI network of targets and DEGs was constructed The top 157 core nodes (F) with a degree value ≥ 70 were used for KEGG (<https://www.kegg.jp/kegg/kegg1.html>) pathway enrichment analysis (G). (H) Sankey diagram were used to shown the components, targets and their associated pathways.

BYF4 and BYF5, with predictions made for 770 targets associated with these compounds. To further analyze these targets' function, we leveraged PPI network and KEGG pathway enrichment to integrate the targets with the differentially expressed genes observed in epithelial cell senescence induced by CSE/LPS. The findings revealed that the compounds contained in BYF4/5 interact with diverse targets that regulated multiple genes, which were mainly related to the p53, FoxO, TNF, NF-kappa B, chemokine, AMPK, Hippo signaling pathway, and cellular senescence, cell cycle, autophagy. Previous studies report that AMPK and SIRT1 can both promote autophagy, to remove the damaged cellular components and maintain cellular homeostasis, which is critical for preventing senescence-related decline^{38,39}. Additionally, AMPK can promote the FoxO3a nuclear localization and transcriptional activity, leading to the expression of genes that promote cell autophagy⁴⁰. In our in vitro studies indicated that hesperidin and nobletin contained in BYF4/5 could suppress the cellular senescence,

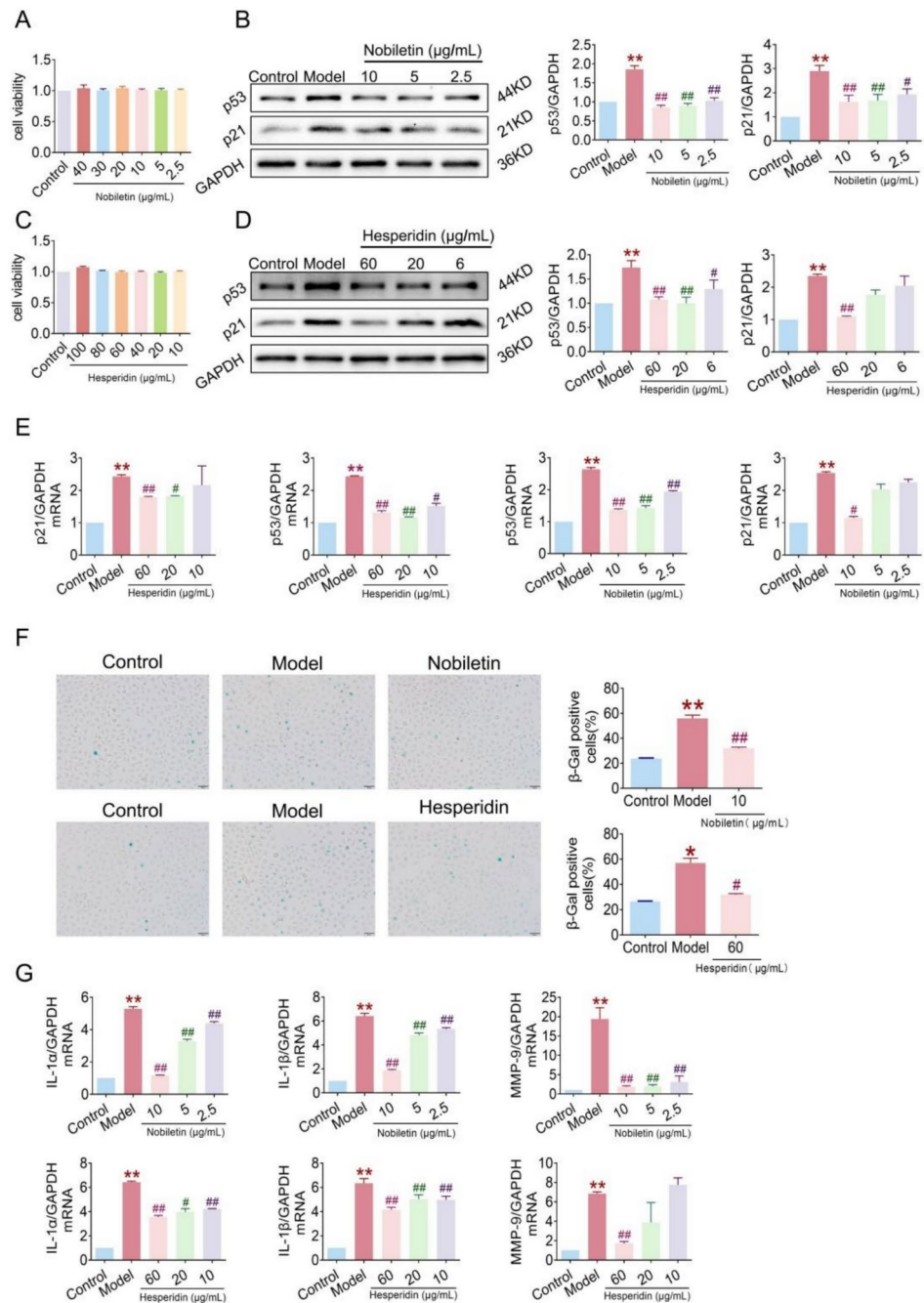


Fig. 9. Nobiletin and hesperidin inhibited cellular senescence and activated AMPK-Sirt1-foxO3a-mediated autophagy. 16-HBE cells were treated with nobiletin or hesperidin for 3 h, and then challenged with CSE/LPS for 24 h. The impact of Nobiletin (A) and hesperidin (C) on cell viability. (B, D) Protein levels of p53 and p21. (E) The mRNA levels of p53 and p21. (F) The activity of β -galactosidase. (G) The mRNA levels of IL-1 α , IL-1 β and MMP-9. Values are expressed as the mean \pm SEM (n = 3), *P < 0.05, **P < 0.01 compared with the control group; #P < 0.05, ##P < 0.01 compared with the model group.

and upregulate the phosphorylated AMPK, Sirt1, and LC3B II, while downregulating FoxO3a phosphorylation, enhancing its nuclear localization and transcriptional activity. In this study, we found that the active components of BYF, hesperidin and nobiletin, can activate the AMPK-Sirt1 pathway to enhance cellular autophagy and mitigate senescence. Previous studies indicate that hesperidin exhibits anti-senescence properties by inhibiting IL-6/STAT3 signaling in pulmonary fibrosis⁴¹, while also demonstrating anti-inflammatory, antioxidant, and anticancer effects through modulation of endothelial function and cell cycle regulation⁴². Nobiletin has been shown to induce autophagy-dependent cell death in gastric cancer via PI3 K/Akt/mTOR signaling⁴³, and it exerts anti-inflammatory and metabolic regulatory effects by targeting oxidative stress and inflammation in respiratory and liver diseases⁴⁴, highlighting its potential in combating apoptosis, autophagy dysregulation,

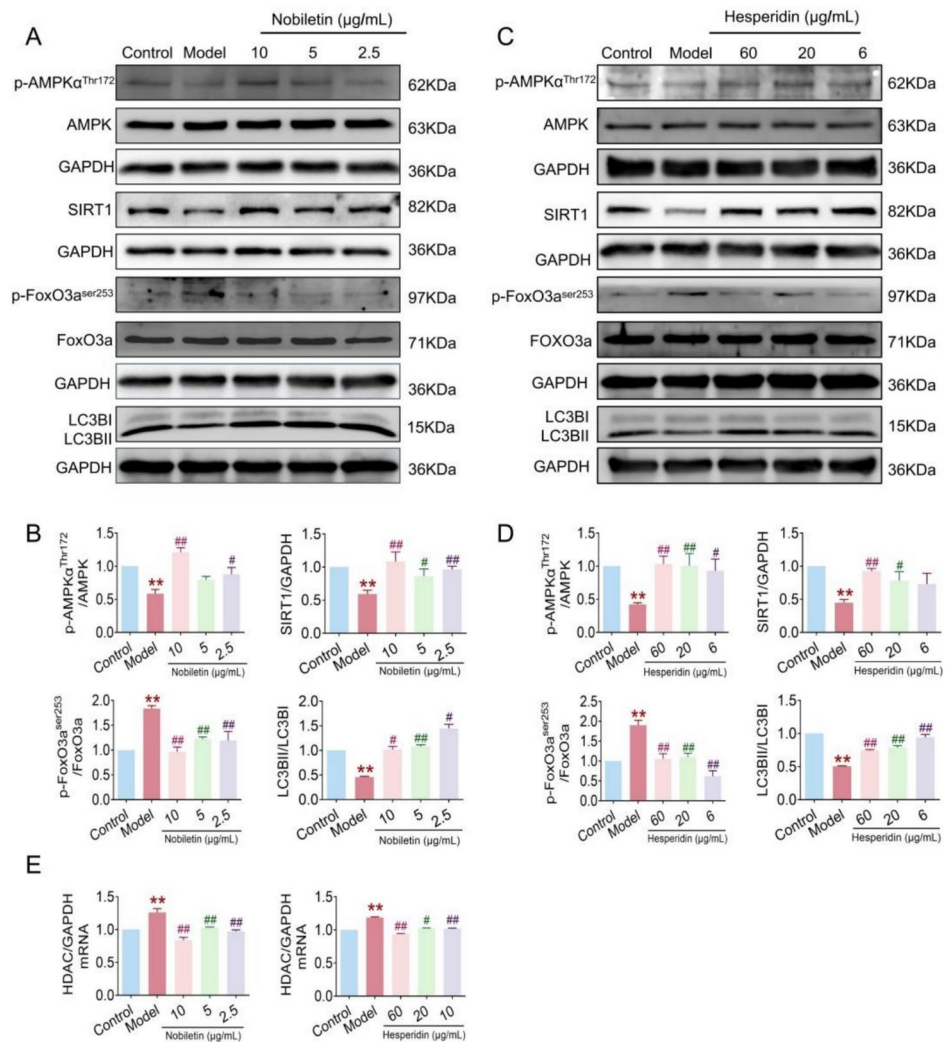


Fig. 10. Nobiletin and hesperidin inhibited cellular senescence and activated AMPK-Sirt1-foxO3a-mediated autophagy. 16-HBE cells were treated with nobiletin or hesperidin for 3 h, and then challenged with CSE/LPS for 24 h. (A–D) Protein levels of phosphorylated AMPK, Sirt1 and FoxO3a. (E) The mRNA levels of HDAC. Values are expressed as the mean \pm SEM (n = 3), *P < 0.05, **P < 0.01 compared with the control group; #P < 0.05, ##P < 0.01 compared with the model group.

and senescence-associated conditions. However, the specific target proteins of hesperidin and nobiletin remain unclear, and further research is needed to elucidate how they activate the AMPK-Sirt1 pathway to enhance cellular autophagy and improve senescence in vivo.

Conclusions

This study demonstrated that BYF treatment mitigated pulmonary function decline, lung pathological changes, inflammatory responses, and protease imbalance in COPD rats, likely by alleviating airway epithelial cell senescence. Additionally, chemical analysis, network pharmacology, and transcriptomics revealed that BYF contains various compounds that bind to multiple targets which might be associated with regulating AMPK, Sirt1, FoxO, and autophagy. In vivo study also demonstrated that hesperidin and nobiletin in BYF4/5 can suppress cellular senescence by upregulating phosphorylated AMPK, Sirt1, and LC3B II, while downregulating FoxO3a phosphorylation, thereby enhancing its nuclear localization and transcriptional activity.

Materials and methods

Animals

48 male Sprague–Dawley rats (6–8 weeks, 220 \pm 20 g), and obtained from Beijing Weitong Lihua Co., Ltd. (License Number: SCXK (Beijing) 2016–0011), were housed in an environment maintained at a temperature of 25 \pm 1 $^{\circ}$ C, with a relative humidity level ranging from 50 \pm 10%, air exchange rate of 10–15 times/hour. The rats were provided with sterilized feed and water. Regular checks were conducted on the purification system to ensure a tranquil environment. The animal protocols were approved by the Animal Ethics Committee of

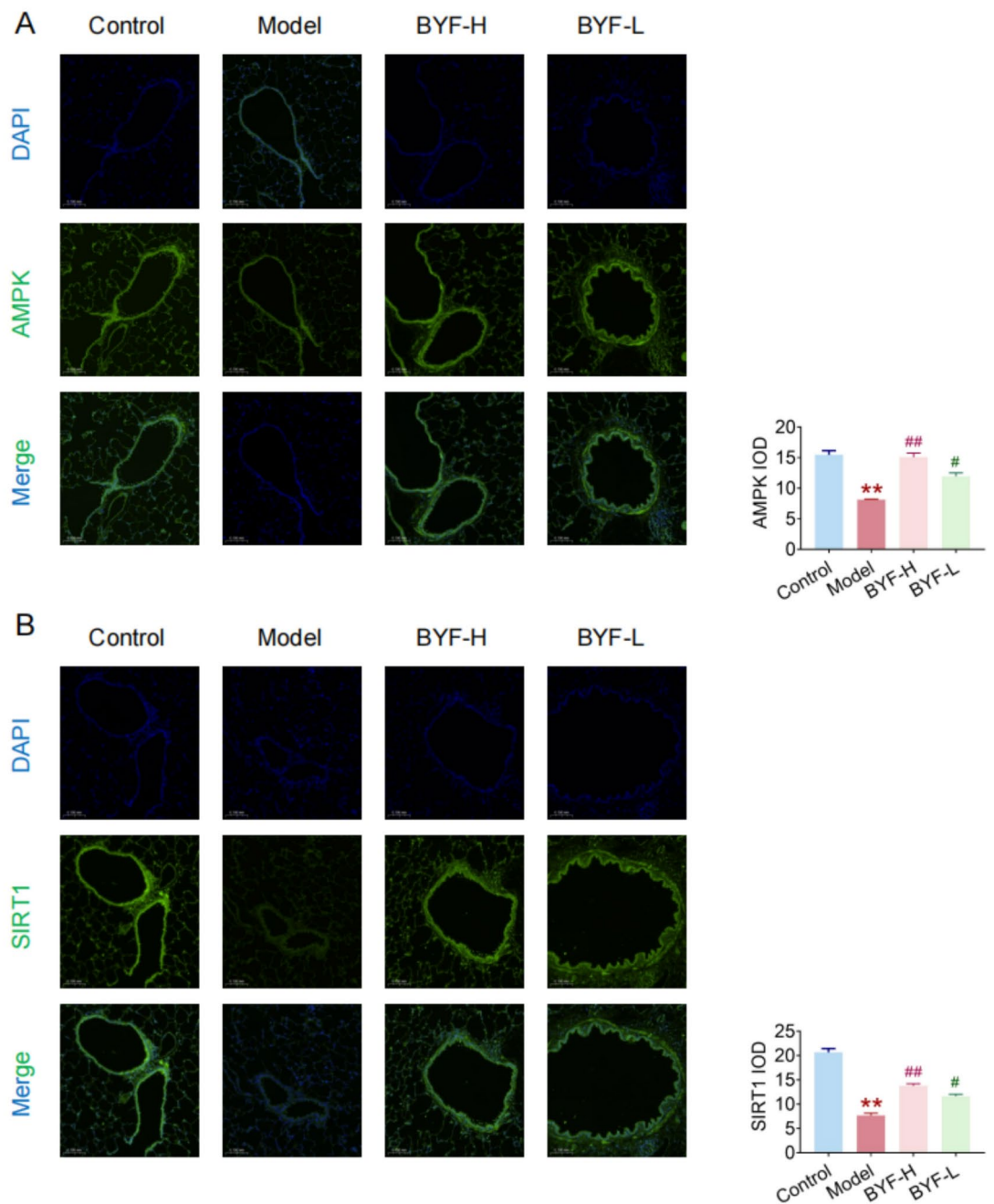


Fig. 11. Effect of Bufei Yishen formula on the protein levels of AMPK and SIRT1 in the lung tissues of COPD rats. Immunofluorescence staining was applied to detect the AMPK (A), SIRT1 (B), in lung tissues.

Henan University of Chinese Medicine (DWLL202003210). We report the use of live animals in accordance with the ARRIVE guidelines (PLoS Biol 8(6): e1000412, 2010) and confirm that all experiments were conducted in compliance with relevant guidelines and regulations⁴⁵.

COPD rat model and drug administration

The forty rats were allocated into five groups: Control group, Model group, Bufei Yishen formula high-dose group (BYF-H), Bufei Yishen formula low-dose group (BYF-L), and N-acetylcysteine group (NAC). From weeks 1 to week 8, rats were exposed to cigarette smoke and bacterial infection to establish a COPD rat model⁴⁶. Briefly, a solution containing *Klebsiella pneumoniae* (6×10^7 CFU/100 μ L/rat, National Center for Medical Culture Collection, Beijing, China, ID: 46,117) was administered intranasally to the rats once every 5 days. Concurrently, the smoke concentration in the exposure chamber was adjusted to (3000 ± 500) PPM twice daily.

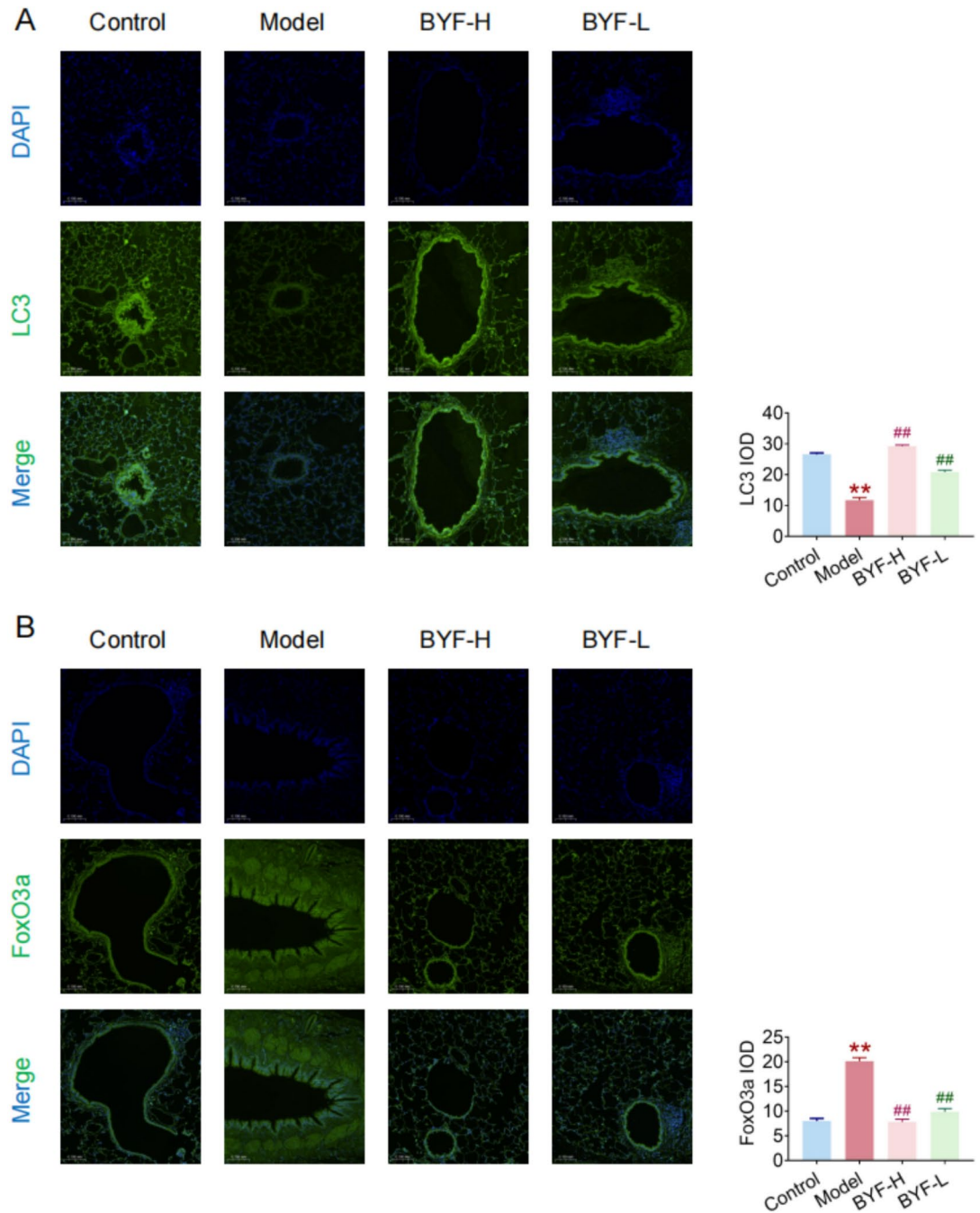


Fig. 12. Effect of Bufei Yishen formula on the protein levels of LC3 and FoxO3a in the lung tissues of COPD rats. Immunofluorescence staining was applied to detect the LC3 (A), FoxO3a (B), in lung tissues.

for a duration of 40 min each session, with a minimum interval of 3 h between the two smoking sessions (once in the morning and once in the evening).

The drugs (BYF: 5.8, 11.6 g/kg/d; NAC: 54 mg/kg/d) were administered via gavage starting at the beginning of the 9th week. The dosage for rats was determined using the following formula: $D_{rat} = D_{human} \times (K_{rat}/K_{human}) \times (W_{rat}/W_{human})^{2/3}$. Here, D represents the dose; K is the body type index, calculated as $K = A/W^{2/3}$ (where A is the surface area/m² and W is the body mass/kg). The Control group and the Model group received an oral administration of a solvent containing 0.5% carboxymethyl cellulose sodium (CMC-Na) at a dosage of 5 mL/kg/d⁴⁷. The rats were euthanized on the first day of the 17th week with a 2% pentobarbital sodium solution (40 mg/kg).

BYF preparation

The BYF extract was prepared by decocting Astragali Radix, Lycii Fructus, Epimedii Herba, Paeoniae Rubra Radix, and Pheretima in water for two cycles. Concurrently, Ginseng Radix Et Rhizoma, Ardisiae Japonicae

No	Herbal drug	Latin scientific name	Plant part(s)	Chemical compounds	Amount (g)
1	Ginseng Radix et Rhizoma	<i>Panax ginseng</i> C.A. Mey	Radix et Rhizoma	ginsenoside Rb1, ginsenoside Rd, pseudoginsenoside	9
2	Astragali Radix	<i>Astragalus tibetanus</i> Bunge	Radix	Astragaloside, calycosin, formononetin	15
3	Corni Fructus	<i>Cornus officinalis</i> Siebold & Zucc	Fructus	ursolic acid, Loganin	12
4	Lycii Fructus	<i>Lycium barbarum</i> L	Fructus	Cyanin, glycitein, fucosterol,	12
5	Schisandrae Chinensis Fructus	<i>Schisandra arisanensis</i> Hayata	Fructus	deoxyschizandrin Schisandrin, Schisandrin B	9
6	Fritillariae Thunbergii Bulbus	<i>Fritillaria thunbergii</i> Miq	Bulbus	Peiminoside, peimisine, pelargonidin	9
7	Perillae Fructus	<i>Perilla frutescens</i> (L.) Britton	Fructus	Luteolin, spinasterol, obtusifoliol	9
8	Citri Reticulatae Pericarpium	<i>Citrus sinensis</i> (L.) Osbeck	Pericarpium	Nobiletin, Hesperidin	9
9	Epimedii Folium	<i>Epimedium acuminatum</i> Franch	Folium	Epimedin A, Epimedin B, Epimedin C icaraside I, Hyperin	9
10	Paeoniae Rubra Radix	<i>Paeonia anomala</i> L	Radix	paeoniflorin	9
11	pheretima	<i>Pheretima aspergillum</i> (E. Perrier)		Lumbrofebrine, lumbricitin	12
12	Ardisiae Japonicae Herba	<i>Ardisia japonica</i> (Thumb.) Blume	Herba	bergenin Kaempferol	15

Table 1. The compositions and chemical compounds of Bufei Yishen formula.

No	Herbal drug	Production company	Lot number	place of origin
1	Ginseng Radix et Rhizoma	Ruilong Pharmaceutical	23,040,101	Ji Lin, China
2	Astragali Radix	Ruilong Pharmaceutical	20,100,102	Nei Mongol, China
3	Corni Fructus	Ruilong Pharmaceutical	220,301,012	Henan, China
4	Lycii Fructus	Ruilong Pharmaceutical	22,100,102	Ningxia, China
5	Schisandrae Chinensis Fructus	Ruilong Pharmaceutical	22,040,101	Liaoning, China
6	Fritillariae Thunbergii Bulbus	Ruilong Pharmaceutical	22,100,102	Zhejiang, China
7	Perillae Fructus	Shenglin Pharmaceutical Co., LTD	CP-464-211,201	Lingchuan, China
8	Citri Reticulatae Pericarpium	Ruilong Pharmaceutical	22,070,102	Hubei, China
9	Epimedii Folium	Anguo Runde Pharmaceutical Co., LTD	C22062208	Gansu, China
10	Paeoniae Rubra Radix	Ruilong Pharmaceutical	141,101	Hebei, China
11	pheretima	Ruilong Pharmaceutical	18,060,205	Guangdong, China
12	Ardisiae Japonicae Herba	Zhangshu Tianqitang Chinese Medicine slices Co., LTD	1,711,006	Jiangxi, China

Table 2. The origin and lot number of the drugs in Bufei Yishen prescription.

Herba, Corni Fructus, Fritillariae Thunbergii Bulbus, Perillae Fructus, Schisandrae Chinensis Fructus, and Citri Reticulatae Pericarpium were extracted twice using 70% ethanol (Table 1, 2). The collection and preparation of all drugs used in the experiment adhered to the guidelines outlined in the Chinese Pharmacopoeia (2020 Edition). These Chinese herbal medicines were authenticated by Professor Fuyu from the School of Pharmacy at Henan University of Chinese Medicine and samples were retained. The resulting extracts were filtered, concentrated, and dried to obtain a dry powder containing 2.59 g of Chinese herbs per gram of powder. This powder was dissolved in double-distilled water (0.22 g/ml) and orally administered to rats.

The BYF dry powder (5 g) was dissolved in methanol or distilled water and mixed with macroporous resin, which was left in the column overnight. The column was then washed sequentially with 0%, 10%, 30%, 60%, 90%, and 100% ethanol solutions. These six fractions were freeze-dried into powder, and subsequently dissolved in dimethyl sulfoxide (100 mg/ml) for in vitro experiments³⁷.

Pulmonary function

Pulmonary function was assessed every four weeks from baseline to week 16. This was done using whole-body plethysmography (WBP, Buxco Inc., Wilmington, NC, USA) to measure tidal volume (TV), peak expiratory flow (PEF), minute ventilation (MV), and expiratory flow at 50% of tidal volume (EF50).

Histological analyses

The left lung lobe was immersed in 10% neutral buffered formalin for 72 h. A 3 mm section near the lung hilum was embedded in paraffin, sectioned into 4 µm-thick sections, and stained with Mayer's hematoxylin and 1% eosin alcohol solution (H&E staining). Adobe Photoshop CC software's counting tool was used to measure the Mean Alveolar Number (MAN/mm²) and Mean Linear Intercept (MLI, µm). Immunohistochemical staining (IHC) quantified the expression levels of SOD2, IL-6, IL-1β, TNF-α, MMP-2, and MMP-9 in lung tissue. To deactivate endogenous peroxidase activity, lung tissue sections were immersed in citrate buffer and incubated in 5% BSA solution for 30 min. The sections were then treated overnight at 4°C with primary polyclonal antibodies, followed by incubation with an HRP-labeled secondary antibody for 20 min at 37°C. Tissue sections were ultimately stained with diaminobenzidine (DAB) solution (Servicebio, Wuhan, China). Hematoxylin from

Solarbio was used as a counterstain to facilitate subsequent restaining. Image-Pro Plus 6.0 software was used for a comprehensive analysis to measure the integrated optical density (IOD) of the samples.

Immunofluorescence analysis

After dewaxing, dehydration, and fixation, the sections were incubated at 37 °C with 5% BSA for 30 min. Subsequently, the samples were incubated with antibodies against Ki67, SP-A, PINK1, FoxO3a, LC3, SIRT1, AMPK, γ -H2 A.X, TUNEL, and p21 (1:200) at 4 °C overnight, followed by a 50-min incubation with secondary antibodies. The nuclei were counterstained with DAPI. Finally, images were captured using CaseViewer software.

Cells were fixed with 4% paraformaldehyde, permeabilized with 0.3% TritonX-100, and blocked with 10% normal goat serum. Subsequently, they were incubated with antibodies against p21 and p53 at 4 °C overnight, followed by incubation with secondary antibodies for 2 h at room temperature. Finally, cell nuclei were labeled using DAPI stain. Images were observed using the OLYMPUS confocal fluorescence microscopy imaging system.

Enzyme-linked immunosorbent assay (ELISA)

The expression levels of the inflammatory factors IL-1 β (RD, DY501), IL-6(BD, 550,319, TNF- α (BD, 558,535), MMP-9, MMP-2, and SOD2 in lung tissue and serum were measured using an ELISA kit.

Cell culture and treatment

The 16HBE cell line was cultured in DMEM (Solarbio, Science & Technology Co., Ltd., Beijing, China) supplemented with 10% FBS (OriCell, Cat. NO. FBSST-01033–500) at 37 °C with 5% CO₂. A total of 2 × 10⁵ cells were plated into 35 mm dishes. The cells were then exposed to drugs for 3 h, and followed by a challenge with CSE (10% concentration) and LPS (100 ng/mL) for 24 hours⁴⁸.

Western blot assay (WB)

The proteins were harvested using RIPA lysate, and their concentrations were detected using the BCA method. The proteins were then separated by 10% SDS-PAGE, transferred onto a PVDF membrane, and blocked with 5% skimmed milk. The membranes were incubated with primary antibodies, including p21waf1/CIP1 (2947S, CST), p-AMPK α Thr172 (2535, CST), p-FoxO3aser253 (9466, CST), LC3B (GTX127375, GeneTex), FoxO3a (GTX100277, GeneTex), p53(10,442–1-AP, Proteintech), AMPK(10,929–2-AP, Proteintech), SIRT (13,161–11-AP, Proteintech), ZO-1(21,773–1-AP, Proteintech), OCC(27,260–1-AP, Proteintech), E-CAD(20,874–1-AP, Proteintech), or GAPDH (10,494 –11-AP, Proteintech), overnight at 4 °C. The membranes were then incubated with secondary antibodies. After washing, the membranes were scanned and analyzed using Image J.

Real-time QPCR analysis (PCR)

RNA was isolated from 16HBE cells using QIAzol reagent (79,306, Qiagen, CA, USA). cDNA synthesis was performed using HiScript II Q RT SuperMix (Vazyme, Nanjing, China), followed by quantification with ChamQ Universal SYBR Master Mix (Vazyme, Nanjing, China).

Senescence-associated β -galactosidase (SA- β -Gal) analysis

The SA- β -Gal staining was performed using an In Situ β -Galactosidase Staining Kit (C0602, Beyotime, China). Cells were fixed with a fixative solution for 10 min at room temperature, followed by three washes with PBS. Subsequently, the cells were incubated in 1 mL of β -Gal staining solution overnight at 37 °C.

Cell viability assay (MTT)

Cell viability and drug toxicity were assessed using the MTT assay. A total of 1 × 10⁵ cells per well were seeded into 96-well plates. BYF, nobiletin, and hesperidin at various concentrations were administered 24 h later. Following another 24-h incubation, the cells were exposed to yellow tetrazolium salt (MTT), which is metabolized by mitochondrial dehydrogenase to form purple formazan crystals. After incubation, the formazan product was dissolved in DMSO, and absorbance was measured spectrophotometrically at 570 nm.

Network pharmacology and transcriptomics analysis

Screening of potential targets of BYF

UPLC-Q/TOF-MS/MS was utilized to identify the constituents of BYF4/5. The potential targets of these identified compounds were predicted using the Swiss Target Prediction Database. Subsequently, Cytoscape v3.9.1 software was used to visualize interactions between the compounds and their predicted targets.

Transcriptomics analysis

Total RNA was extracted from 16HBE cells using TRIZOL reagent (Invitrogen, Carlsbad, CA, USA) following the manufacturer's protocol. RNA sequencing (RNA-seq) was then performed to identify differentially expressed genes (DEGs) in 16HBE cells treated with CSE/LPS. DEGs were defined based on a significance level of p-value < 0.05 and an absolute |log₂ FC| > 1.

Protein-Protein Interaction and KEGG pathway analysis

The protein-protein interaction network of the target proteins and differentially expressed genes (DEGs) was constructed using the STRING database and Cytoscape v3.9.1 software. KEGG (<https://www.kegg.jp/kegg/kegg1.html>) pathway enrichment analysis of the core nodes (degree value \geq 70) was conducted using the STRING database^{49–51}.

Statistical analysis

Statistical analyses were performed using one-way analysis of variance (ANOVA). The Least Significant Difference (LSD) test was employed for homogeneity of variance, while Dunnett's T3 method was used for heterogeneity of variance. Data are presented as mean \pm SEM. A $P < 0.05$ was considered statistically significant.

Data availability

Data is provided within the manuscript or supplementary information files.

Received: 16 June 2024; Accepted: 30 April 2025

Published online: 13 May 2025

References

- Venkatesan, P. GOLD COPD report: 2024 update. *Lancet Respir. Med.* **12**, 15–16 (2024).
- Iheanacho, I., Zhang, S., King, D., Rizzo, M. & Ismaila, A. S. Economic Burden of Chronic Obstructive Pulmonary Disease (COPD): A Systematic Literature Review. *COPD* **15**, 439–460 (2020).
- Zuo, L. & Wijegunawardana, D. Redox Role of ROS and Inflammation in Pulmonary Diseases. In *Lung Inflammation in Health and Disease, Volume II* (ed. Wang, Y. X.) 187–204 (Springer International Publishing, 2021). https://doi.org/10.1007/978-3-030-68748-9_11.
- Aydemir, Y. et al. Comparison of oxidant/antioxidant balance in COPD and non-COPD smokers. *Heart Lung* **48**, 566–569 (2019).
- Gouda, M. M., Shaikh, S. B. & Bhandary, Y. P. Inflammatory and Fibrinolytic System in Acute Respiratory Distress Syndrome. *Lung* **196**, 609–616 (2018).
- Carlier, F. M., De Fays, C. & Pilette, C. Epithelial Barrier Dysfunction in Chronic Respiratory Diseases. *Front. Physiol.* **12**, 619227 (2021).
- Gao, W. et al. Bronchial epithelial cells: The key effector cells in the pathogenesis of chronic obstructive pulmonary disease?. *Respirology* **20**, 722–729 (2015).
- Shaikh, S. B., Goracci, C., Tjitropranoto, A. & Rahman, I. Impact of aging on immune function in the pathogenesis of pulmonary diseases: Potential for therapeutic targets. *Expert Rev. Respir. Med.* **17**, 351–364 (2023).
- Kumar, M., Seeger, W. & Voswinckel, R. Senescence-Associated Secretory Phenotype and Its Possible Role in Chronic Obstructive Pulmonary Disease. *Am. J. Respir. Cell Mol. Biol.* **51**, 323–333 (2014).
- Bateman, G. et al. Airway Epithelium Senescence as a Driving Mechanism in COPD Pathogenesis. *Biomedicines* **11**, 2072 (2023).
- Suryadevara, V. et al. SenNet recommendations for detecting senescent cells in different tissues. *Nat. Rev. Mol. Cell Biol.* <https://doi.org/10.1038/s41580-024-00738-8> (2024).
- Gouda, M. M. et al. Changes in the expression level of IL-17A and p53-fibrinolytic system in smokers with or without COPD. *Mol. Biol. Rep.* **45**, 2835–2841 (2018).
- Huang, W.-J., Fan, X.-X., Yang, Y.-H., Zeng, Y.-M. & Ko, C.-Y. A review on the Role of Oral Nutritional Supplements in Chronic Obstructive Pulmonary Disease. *J. Nutr. Health Aging.* **26**, 723–731 (2022).
- Han, Y. et al. The Role and Application of the AMPK-Sirtuins Network in Cellular Senescence. *Front. Biosci. (Landmark Ed)* **28**, 250 (2023).
- Tabibzadeh, S. Signaling pathways and effectors of aging. *Front. Biosci.* **26**, 50–96 (2021).
- Lee, S.-H., Lee, J.-H., Lee, H.-Y. & Min, K.-J. Sirtuin signaling in cellular senescence and aging. *BMB Rep.* **52**, 24–34 (2019).
- Yuan, D. et al. Senescence associated long non-coding RNA 1 regulates cigarette smoke-induced senescence of type II alveolar epithelial cells through sirtuin-1 signaling. *J. Int. Med. Res.* **49**, 030006052098604 (2021).
- Shaikh, S. B., Prabhu, A. & Bhandary, Y. P. Targeting anti-aging protein sirtuin (Sirt) in the diagnosis of idiopathic pulmonary fibrosis. *J. Cell. Biochem.* **120**, 6878–6885 (2019).
- Li, S. et al. Effects of comprehensive therapy based on traditional Chinese medicine patterns in stable chronic obstructive pulmonary disease: A four-center, open-label, randomized, controlled study. *BMC Complement Altern. Med.* **12**, 197 (2012).
- Zhao, P. et al. Restoring Th17/Treg balance via modulation of STAT3 and STAT5 activation contributes to the amelioration of chronic obstructive pulmonary disease by Bufeif Yishen formula. *J. Ethnopharmacol.* **217**, 152–162 (2018).
- Li, J. et al. A chinese herbal formula ameliorates COPD by inhibiting the inflammatory response via downregulation of p65, JNK, and p38. *Phytomedicine* **83**, 153475 (2021).
- Jia, L. et al. Bufeif Yishen formula protects the airway epithelial barrier and ameliorates COPD by enhancing autophagy through the Sirt1/AMPK/Foxo3 signaling pathway. *Chin. Med.* **19**, 32 (2024).
- Yin, P. et al. A Subnational Analysis of Mortality and Prevalence of COPD in China From 1990 to 2013: Findings From the Global Burden of Disease Study 2013. *Chest* **150**, 1269–1280 (2016).
- Li, J. et al. The effective evaluation on symptoms and quality of life of chronic obstructive pulmonary disease patients treated by comprehensive therapy based on traditional Chinese medicine patterns. *Complement. Ther. Med.* **21**, 595–602 (2013).
- Yu, X.-Q. et al. Bu-Fei Yi-Shen Granules Reduce Acute Exacerbations in Patients with GOLD 3–4 COPD: A Randomized Controlled Trial. *Int. J. Chron. Obstruct. Pulmon. Dis.* **18**, 2439–2456 (2023).
- Wang, C. et al. Prevalence and risk factors of chronic obstructive pulmonary disease in China (the China Pulmonary Health [CPH] study): A national cross-sectional study. *Lancet* **391**, 1706–1717 (2018).
- Zhang, L. et al. Cellular senescence: A key therapeutic target in aging and diseases. *J. Clin. Investig.* **132**, e158450 (2022).
- Roger, L., Tomas, F. & Gire, V. Mechanisms and Regulation of Cellular Senescence. *IJMS* **22**, 13173 (2021).
- Ohtani, N. & Hara, E. Roles and mechanisms of cellular senescence in regulation of tissue homeostasis. *Cancer Sci.* **104**, 525–530 (2013).
- Woldhuis, R. R. et al. Link between increased cellular senescence and extracellular matrix changes in COPD. *Am. J. Physiol.-Lung Cell. Mol. Physiol.* **319**, L48–L60 (2020).
- Aghali, A., Koloko Ngassie, M. L., Pabelick, C. M. & Prakash, Y. S. Cellular Senescence in Aging Lungs and Diseases. *Cells* **11**, 1781 (2022).
- Birch, J., Barnes, P. J. & Passos, J. F. Mitochondria, telomeres and cell senescence: Implications for lung ageing and disease. *Pharmacol. Ther.* **183**, 34–49 (2018).
- Cai, Q., Chen, S., Zhu, Y. & Li, Z. Knockdown of GNL3L Alleviates the Progression of COPD Through Inhibiting the ATM/p53 Pathway. *COPD* **18**, 2645–2659 (2023).
- Levi, N. et al. p21 facilitates chronic lung inflammation via epithelial and endothelial cells. *Aging* **15**, 2395–2417 (2023).
- Raby, K. L., Michaeloudes, C., Tonkin, J., Chung, K. F. & Bhavsar, P. K. Mechanisms of airway epithelial injury and abnormal repair in asthma and COPD. *Front. Immunol.* **14**, 1201658 (2023).
- Wei, Y. et al. Maintenance of airway epithelial barrier integrity via the inhibition of AHR/EGFR activation ameliorates chronic obstructive pulmonary disease using effective-component combination. *Phytomedicine* **118**, 154980 (2023).
- Wu, J. et al. Chemical Identification and Antioxidant Screening of Bufeif Yishen Formula using an Offline DPPH Ultrahigh-Performance Liquid Chromatography Q-Extractive Orbitrap MS/MS. *Int. J. Anal. Chem.* **2022**, 1–19 (2022).

38. Sánchez, B., Muñoz-Pinto, M. F. & Cano, M. AMPK, autophagy and telomerase. *Expert Reviews in Molecular Medicine*.
39. Yang, L., Shi, J., Wang, X. & Zhang, R. Curcumin Alleviates D-Galactose-Induced Cardiomyocyte Senescence by Promoting Autophagy via the SIRT1/AMPK/mTOR Pathway. *Evid.-Based Complement. Altern. Med.* **2022**, 1–11 (2022).
40. Dai, B. et al. ASIC1a Promotes Acid-Induced Autophagy in Rat Articular Chondrocytes through the AMPK/FoxO3a Pathway. *IJMS* **18**, 2125 (2017).
41. Han, D. et al. Hesperidin inhibits lung fibroblast senescence via IL-6/STAT3 signaling pathway to suppress pulmonary fibrosis. *Phytomedicine* **112**, 154680 (2023).
42. Imperatrice, M., Cuijpers, I., Troost, E. J. & Stijns, M. M. J. P. E. Hesperidin Functions as an Ergogenic Aid by Increasing Endothelial Function and Decreasing Exercise-Induced Oxidative Stress and Inflammation, Thereby Contributing to Improved Exercise Performance. *Nutrients* **14**, 2955 (2022).
43. Chen, M. et al. Nobiletin targets SREBP1/ACLY to induce autophagy-dependent cell death of gastric cancer cells through PI3K/Akt/mTOR signaling pathway. *Phytomedicine* **128**, 155360 (2024).
44. Fan, C. et al. Nobiletin Ameliorates Hepatic Lipid Deposition, Oxidative Stress, and Inflammation by Mechanisms That Involve the Nrf2/NF- κ B Axis in Nonalcoholic Fatty Liver Disease. *J. Agric. Food Chem.* **71**, 20105–20117 (2023).
45. Sert, P. D. et al. The ARRIVE guidelines 20: Updated guidelines for reporting animal research. *PLoS Biol* **18**, e3000410 (2020).
46. Li, Y. et al. A Rat Model for Stable Chronic Obstructive Pulmonary Disease Induced by Cigarette Smoke Inhalation and Repetitive Bacterial Infection. *Biol. Pharm. Bull.* **35**, 1752–1760 (2012).
47. Li, Y. et al. Long-term effects of three Tiao-Bu Fei-Shen therapies on NF- κ B/TGF- β 1/smad2 signaling in rats with chronic obstructive pulmonary disease. *BMC Complement Altern. Med.* **14**, 140 (2014).
48. Yulong, C. et al. Three Tiaobu Feishen therapies protect human alveolar epithelial cells against cigarette smoking and tumor necrosis factor- α -induced inflammation by nuclear factor-kappa B pathway. **39**, (2019).
49. Kanehisa, M., Furumichi, M., Sato, Y., Matsuura, Y. & Ishiguro-Watanabe, M. KEGG: Biological systems database as a model of the real world. *Nucleic Acids Res.* **53**, D672–D677 (2024).
50. Kanehisa, M. Toward understanding the origin and evolution of cellular organisms. *Protein Sci.* **28**, 1947–1951 (2019).
51. Kanehisa, M. & Goto, S. KEGG: Kyoto encyclopedia of genes and genomes. *Nucleic Acids Res.* **28**, 27–30 (2000).

Author contributions

Z.P. and L. J. designed this study. C.M., Y. M. and T. Y. performed the animal experiments. P.Z., and T. Y. drafted and revised the manuscript. L. X. contributed to the data analysis. All authors have read and approved the manuscript.

Funding

Joint Fund for Science and Technology Research of Henan Province, No. 222301420020; Supported by Natural Science Foundation of Henan, No.252300421138; Training Program for Young Teachers in Henan's University, No. 2023GGJS084; Henan Education Science and Technology Innovation Talent Support Program, No. 24HAS-TIT073. Research Projects of Higher Education Institutions in Henan Province, 24A360013.

Declarations

Competing interests

The authors declare no competing interests.

Additional information

Supplementary Information The online version contains supplementary material available at <https://doi.org/10.1038/s41598-025-00746-4>.

Correspondence and requests for materials should be addressed to J.L. or P.Z.

Reprints and permissions information is available at www.nature.com/reprints.

Publisher's note Springer Nature remains neutral with regard to jurisdictional claims in published maps and institutional affiliations.

Open Access This article is licensed under a Creative Commons Attribution-NonCommercial-NoDerivatives 4.0 International License, which permits any non-commercial use, sharing, distribution and reproduction in any medium or format, as long as you give appropriate credit to the original author(s) and the source, provide a link to the Creative Commons licence, and indicate if you modified the licensed material. You do not have permission under this licence to share adapted material derived from this article or parts of it. The images or other third party material in this article are included in the article's Creative Commons licence, unless indicated otherwise in a credit line to the material. If material is not included in the article's Creative Commons licence and your intended use is not permitted by statutory regulation or exceeds the permitted use, you will need to obtain permission directly from the copyright holder. To view a copy of this licence, visit <http://creativecommons.org/licenses/by-nc-nd/4.0/>.

© The Author(s) 2025